Solid State Ionics 192 (2011) 677–681

Contents lists available at ScienceDirect

Solid State Ionics

journal homepage: www.elsevier.com/locate/ssi

# Oxygen permeability and stability of asymmetric multilayer $Ba_{0.5}Sr_{0.5}Co_{0.8}Fe_{0.2}O_{3-\delta}$ ceramic membranes

A.V. Kovalevsky [a,*], A.A. Yaremchenko [b], V.A. Kolotygin [b], F.M.M. Snijkers [c], V.V. Kharton [b], A. Buekenhoudt [a], J.J. Luyten [c]

[a] Conversion and Separation Technology, Flemish Institute for Technological Research (VITO), 2400 Mol, Belgium
[b] Department of Ceramics and Glass Engineering, CICECO, University of Aveiro, 3810-193 Aveiro, Portugal
[c] Materials Department, Flemish Institute for Technological Research (VITO), 2400 Mol, Belgium

ARTICLE INFO

*Article history:*
Received 26 August 2009
Received in revised form 10 May 2010
Accepted 24 May 2010
Available online 18 June 2010

*Keywords:*
Oxygen permeation
BSCF
Mixed ionic–electronic conductor
Asymmetric ceramic membrane
Microstructural stability

ABSTRACT

Perovskite-type $Ba_{0.5}Sr_{0.5}Co_{0.8}Fe_{0.2}O_{3-\delta}$ (BSCF) is considered as one of most promising materials for the oxygen separation from air. In order to assess the impact of asymmetric architecture on oxygen transport properties and stability, dense ceramics and membranes consisting of two porous and one dense layers were fabricated and tested. The stability of $Ba_{0.5}Sr_{0.5}Co_{0.8}Fe_{0.2}O_{3-\delta}$ in atmospheres with low oxygen partial pressure is similar to that for $SrCo_{0.8}Fe_{0.2}O_{3-\delta}$. Analysis of the thickness dependence of oxygen permeation fluxes through symmetric dense membranes unambiguously showed that the permeation is limited by surface exchange kinetics at $d \leq 1$ mm. The main limitations for the oxygen permeation through asymmetric membranes are associated with gas diffusion in pores and oxygen desorption process, despite a high open porosity (49%) of the porous layers. The asymmetric membranes demonstrated a stable performance if using inert sweep gas. On exposing to $CO_2/H_2O$ containing atmospheres, the permeation decreases dramatically due to a deep decomposition process on the permeate side, resulting in the formation of carbonates and/or hydroxides causing blocking of oxygen transport.


## 1. Introduction

At present time, mixed ionic and electronic conducting ceramic membranes have become of great interest as potentially economical, clean and efficient means of producing oxygen by separation from air [1,2]. It is generally accepted that the mixed conducting membranes being developed with sufficient durability and reliability have great potential to meet the needs of many segments of the oxygen market. While the search for novel materials with improved transport and mechanical properties is still a major challenge, a number of research efforts funded by both industry and government have also been directed towards optimization of the membrane geometry (planar, tubular, ribbed, etc.) and microstructural parameters. One promising concept to improve both oxygen permeation flux and thermomechanical stability of the ceramic membranes relates to asymmetric configuration comprising a thin dense high-permeable layer applied on a porous support ([2–7] and references therein). Depending upon thickness of the gas-tight layer in such membranes, the performance-determining factors may be associated with bulk ambipolar conductivity, surface exchange, and/or oxygen diffusion in the porous layers. Considering the high level of ionic transport [8–11], perovskite-type $Ba_{0.5}Sr_{0.5}Co_{0.8}Fe_{0.2}O_{3-\delta}$ (BSCF) mixed conductor was chosen as a material for the planar asymmetric membranes for oxygen separation from gas mixtures. The selected membrane concept includes a thin dense layer supported by relatively thick porous one and covered with an additional thin layer. In this configuration, thick porous support is supposed to provide an additional mechanical strength to the whole system, whilst thin porous film may contribute to the activation of the dense layer due to an enlargement of the surface area. The present work was centered on the fabrication and testing of BSCF-based three-layer asymmetric flat membranes in order to assess effects related to the membrane architecture.

## 2. Experimental

BSCF powder was prepared via THE glycine-nitrate process (GNP), a self-combustion technique using nitrates of metal components as an oxidant and glycine as a fuel and chelating agent [12]. SEM inspection of the powder after subsequent annealing at 1173 K for 2 h for removing organic residues shows, however, a high agglomeration of the particles. In order to decrease agglomeration and to provide easier densification of the ceramics during sintering, the powder was subjected to ball-milling. Addition of Degalan P24 (3 wt.%) as a binder was used for further improving the compactability of the powder. In case of porous layer formation, graphite was used as a pore former. The choice of sintering conditions was based on the possibility to obtain maximum density for intermediate thin layer, whilst optimization of graphite content for green porous layers was performed using an empirical approach taking

* Corresponding author. Tel.: +32 474918506; fax: +32 14321186.
*E-mail address:* akavaleuski@cv.ua.pt (A.V. Kovalevsky).

0167-2738/$ – see front matter © 2010 Elsevier B.V. All rights reserved.
doi:10.1016/j.ssi.2010.05.030

into account the corresponding maximum porosity, acceptable pore structure and mechanical strength, the optimization procedure will be analyzed in details in a separate paper.

The flat three-layer asymmetric membranes were fabricated by a three-stage uniaxial compaction procedure. Calculated amount of BSCF powder, containing 4 wt.% of Degalan P24 and 27 wt.% of graphite, was placed into a mold and compacted at 100 MPa to form the thick porous support layer. Then a fixed amount of BSCF, containing 3 wt.% of the binder was added on the top of the first compact, flattened and compacted again at 100 MPa. In this way a green precursor for a thin dense layer was formed. At the final stage, in order to provide the formation of a third thin porous layer, a calculated amount of the powder similar to that in the first case was added into the mold, accurately flattened and the whole structure was then compacted at 300 MPa to form a three-layer asymmetric membrane. Thus prepared green membranes were sintered at 1393 K for 5 h, using heating/cooling rates as slow as 1–2 K/min, in order to suppress possible formation of microcracks and bending. After sintering, the thicknesses of the thick porous support, of the dense layer and of the thin porous layer were 1.05 mm (fixed), 170 μm (fixed) and 30–300 μm, respectively. Corresponding sets of three-layer (3 L) asymmetric membranes with thin porous layer of 30, 60, 100 and 300 μm are further denoted as 3L-170-30, 3L-170-60, 3L-170-100 and 3L-170-300. Also, for the comparative analysis and estimation of surface exchange limitations, symmetric 0.58–2.67 mm thick membranes were compacted at 300 MPa and then sintered in the same conditions.

General characterization included X-ray diffraction (XRD) analysis, scanning electron microscopy coupled with energy-dispersive spectroscopy (SEM/EDS), picnometry, gas-tightness control, mercury intrusion porosimetry, total conductivity vs $p(O_2)$ measurements and determination of the steady-state oxygen permeation fluxes; description of the experimental procedures and equipment can be found elsewhere (Refs. [13–20] and references cited). For all membranes studied in this work, zero level of physical leakages was confirmed under a total pressure gradient of 2–4 atm. Two techniques were used for the determination of steady-state oxygen permeation fluxes at 973–1223 K. In all cases, the oxygen partial pressure at the membrane feed side ($p_2$) was equal to 21.2 kPa (air), the thin porous layer was exposed to the permeate side with oxygen partial pressure $p_1$. The permeation measurements, described elsewhere [13] and referred to as Method 1, were performed using electrochemical cells made of yttria-stabilized zirconia and equipped with an oxygen pump and a sensor. For this technique, the transport of molecular oxygen through the membrane and, then, through internal space of the solid-electrolyte cells is only driven by the oxygen chemical potential gradient created by the electrochemical pump; no sweep gas is supplied onto the membrane surface, whilst the permeate-side gas phase contains only oxygen and traces of air remaining after sealing. For the sake of comparison, another series of measurements was performed under air/Ar, air/$CO_2$ and air/($CO_2 + H_2O$) gradients, supplying the sweep gas mixtures onto the membrane permeate side (Method 2); the experimental setup was described in Ref. [17].

## 3. Results and discussion

XRD analysis confirmed the formation of cubic single-phase $Ba_{0.5}Sr_{0.5}Co_{0.8}Fe_{0.2}O_{3-\delta}$ in the selected sintering conditions (1393 K, 5 h). Basic SEM inspection revealed high quality and low porosity of BSCF ceramics, while no essential inhomogeneities and phase impurities were detected by energy dispersive spectroscopy. Selected sintering conditions allow the formation of gas-tight BSCF ceramics with the density of 91–93% from theoretical.

Fig. 1 shows the approximate stability boundaries at reduced oxygen chemical potentials, evaluated from data on the total conductivity vs $p(O_2)$ dependencies. The oxygen pressure corresponding to a dramatic conductivity drop caused by the phase decomposition was considered as stability limit at a given temperature, in agreement with XRD. As expected, the decomposition of BSCF occurs at oxygen chemical potentials between those for $Co_3O_4$/CoO and CoO/Co boundaries, and close to the latter. BSCF and $SrCo_{0.8}Fe_{0.2}O_{3-\delta}$ demonstrate similar values of low-$p(O_2)$ stability limits and slopes of van't Hoff dependence, log $p(O_2)$ vs. $1/T$, suggesting the same mechanisms of decomposition, which, in the case of $SrCo_{0.8}Fe_{0.2}O_{3-\delta}$, takes place via the formation of Ruddlesden–Popper $Sr_{n+1}(Co,Fe)_nO_z$ phase and CoO [21]. One should note that, although the substitution of $Sr^{2+}$ with $Ba^{2+}$ leads to suppressing of the brownmillerite phase formation at reduced oxygen partial pressures and to higher oxygen permeation fluxes [9–11], the architectural approach including the fabrication of asymmetric structures for BSCF membranes is still needed to achieve kinetic stabilization at low $p(O_2)$ in order to avoid phase decomposition.

Representative SEM micrograph of a sintered 3L-170-60 BSCF membrane is presented in Fig. 2A. Obviously, the selected sintering conditions and the amount of pore-forming agent allow the formation of porous microstructure for top thin and bottom thick support layer. The average pore diameter and open porosity of the BSCF supports, separately fabricated using the same amount of graphite additive and binder, and sintered in similar conditions, were 4.2 μm and 49.2%, correspondingly. SEM inspection of the boundary between dense and porous layers showed the absence of delamination and crack formation, due to similar thermal expansion coefficients of the layers of asymmetric structure.

Fig. 3 presents the temperature dependencies of oxygen permeation fluxes through dense symmetric BSCF membranes without surface modification under a fixed $p(O_2)$ gradient. The membrane thickness dependencies of the permeation fluxes unambiguously show that the permeation is limited by surface exchange kinetics. In particular, at $d \leq 1.0$ mm the fluxes become almost thickness-independent, in agreement with literature data [22]. The kinetic parameters extracted from the permeation data will be analyzed in a separate publication. Notice, however, that the apparent activation energy for the surface exchange of BSCF, estimated by the model [16], is 41 kJ/mol.

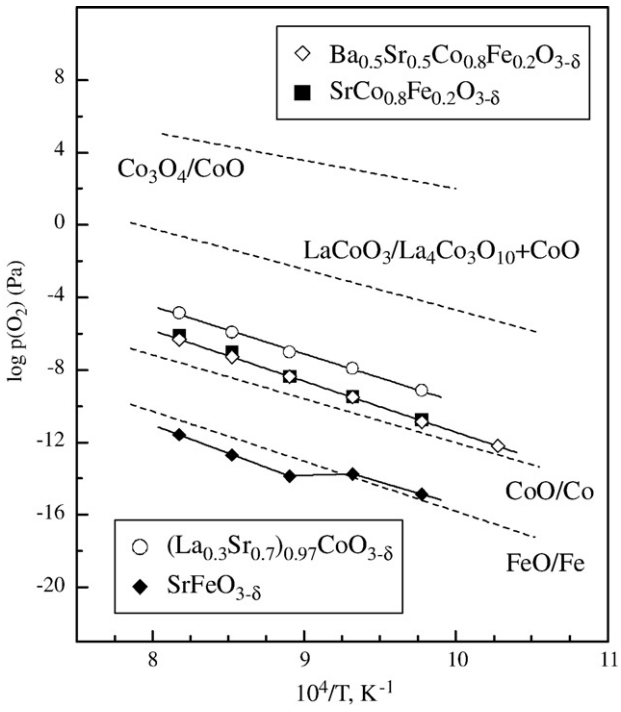


**Fig. 1.** Low-$p(O_2)$ phase stability boundary of $Ba_{0.5}Sr_{0.5}Co_{0.8}Fe_{0.2}O_{3-\delta}$, estimated by the conductivity vs. $p(O_2)$ measurements. Literature data on $SrCo_{0.8}Fe_{0.2}O_{3-\delta}$ [17], $(La_{0.3}Sr_{0.7})_{0.97}CoO_{3-\delta}$ [18], $SrFeO_{3-\delta}$ [19], $LaCoO_{3-\delta}$ [20], $Co_3O_4$ [23], CoO [24] and FeO [24] are shown for comparison.

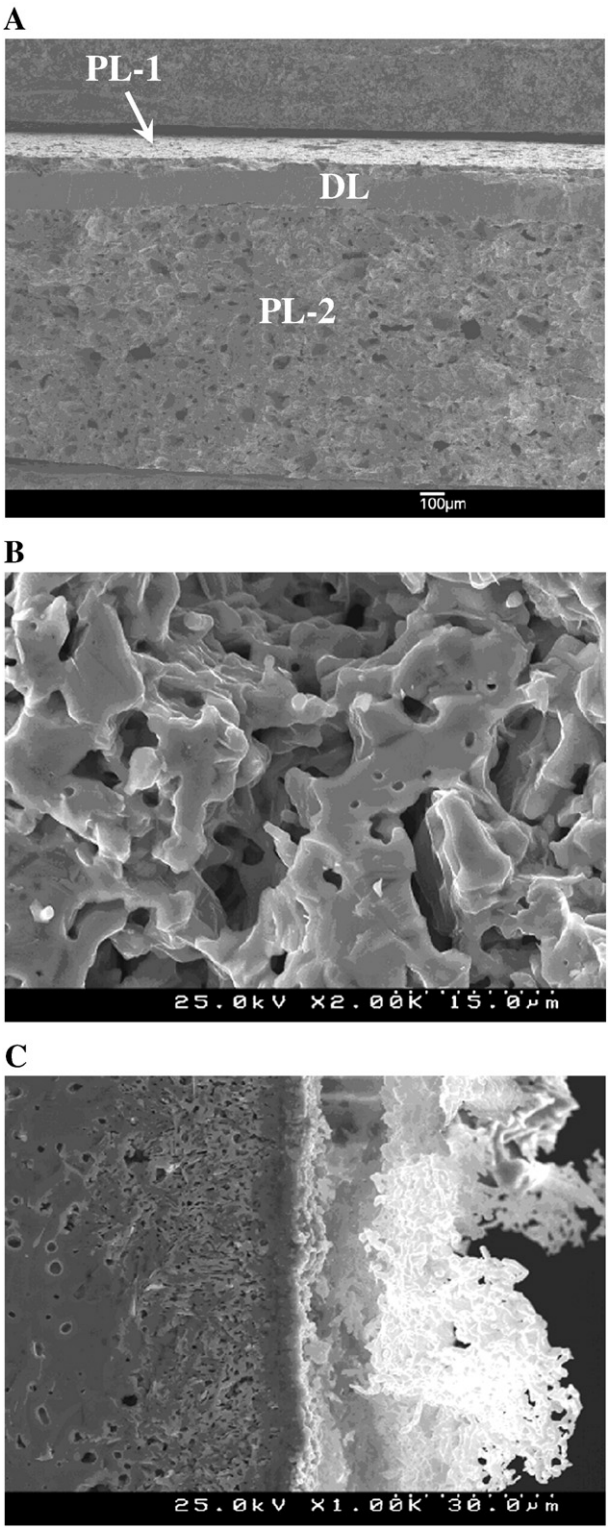


**Fig. 2.** SEM micrographs of a three-layer 3L-170-60 membrane after fabrication (A) and after testing in $CO_2$: surface of the feed-side porous layer (B) and cross-section near the permeate side exposed to $CO_2$ (C). The abbreviations PL-1, DL and PL-2 on micrograph (A) denote thin porous, dense and thick porous support layers, correspondingly. The micrograph (C) shows the dense BSCF layer (left), porous permeate-side layer (center), and carbonate containing layer.

Selected results on the oxygen partial pressure dependence of the oxygen permeation flux through three-layer BSCF membranes, measured by Methods 1 and 2, are shown in Fig. 4. Only a moderate increase in the permeation was observed due to the implementation of

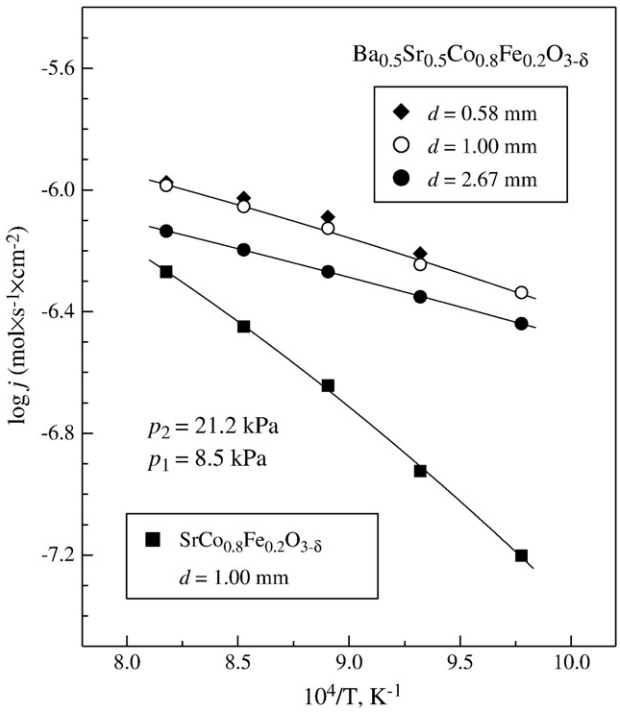


**Fig. 3.** Oxygen permeation fluxes through dense BSCF membranes with different thicknesses under a fixed $p(O_2)$ gradient. Data on $SrCo_{0.8}Fe_{0.2}O_{3-\delta}$ [17] are shown for comparison. All data correspond to membranes without surface modification; the measurements were performed by Method 1.

asymmetric architecture. For instance, the oxygen fluxes through 3L-170-100 membrane at 1223 K were only ~1.5 times higher than those for a 1.00 mm thick symmetric membrane, although one could expect a 5–6 times increase if the surface limitations would be avoided. Apparently, the formation of three-layer membranes leads to an appearance of additional permeation-limiting factor, namely gas diffusion in the porous layers. The measurements performed by Method 1 for 3L-170-100 membrane (Fig. 4A), when no external gas flow is supplied onto the membrane surfaces demonstrate that the fluxes are proportional to $(p_2–p_1)$, clearly indicating that the diffusion of gaseous $O_2$ is among the critical transport-determining factors. The corresponding activation energy, 29 kJ/mol, indicates however that other factors still play a non-negligible role.

When a flowing Ar–$O_2$ mixture is supplied at the permeate-side surface (Fig. 4B), the oxygen fluxes drastically increase, although the $j$ vs. $(p_2–p_1)$ dependencies are still linear. The activation energy increases up to 43 kJ/mol. Since the feed-side surface in these conditions is exposed to a static air atmosphere in both methods, the results show that the permeation through the three-layer membranes is essentially governed by the molecular oxygen diffusion in the pores of the thin layer on the permeate side; supplying sweep gas onto this surface leads to a faster oxygen removal from the pores. As a result, the role of other limiting factors increases. Note that the apparent activation energy becomes similar to that of surface exchange, estimated from the membrane thickness dependence of the permeation fluxes (Fig. 3), thus suggesting an important contribution of the oxygen desorption-related processes.

The obtained data showed that stable and relatively high performance of the asymmetric three-layer membranes can be achieved using an inert sweep gas, such as Ar. In order to assess membrane stability in $CO_2$- and $H_2O$- containing atmospheres, the oxygen permeability of 3L-170-30 and 3L-170-300 membranes was measured separately as a function of time, switching the sweeping gas from argon to carbon dioxide with similar oxygen partial pressure. For $CO_2$/$H_2O$ containing atmospheres oxygen permeation fluxes decrease dramatically

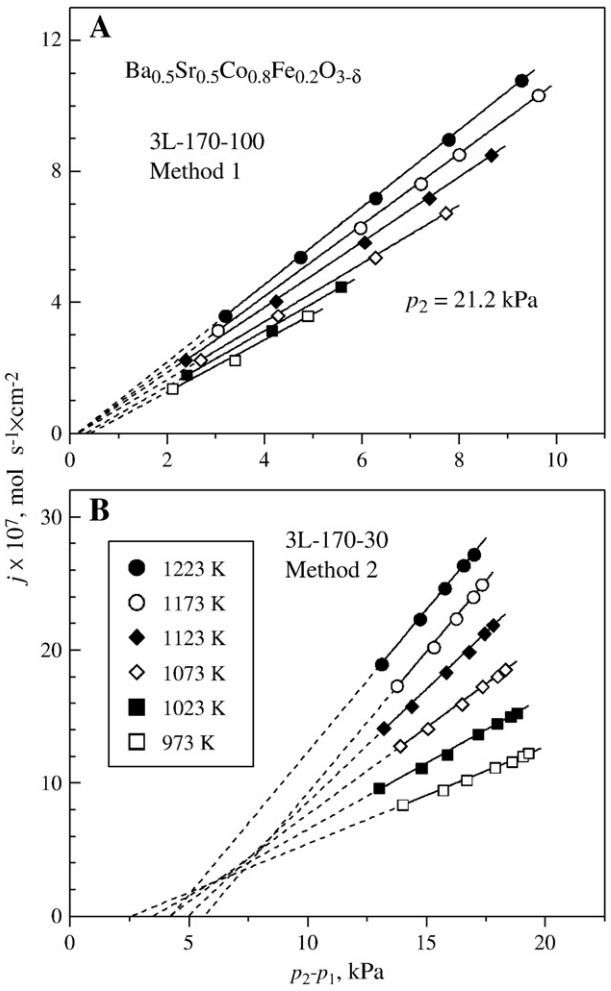


**Fig. 4.** Dependence of oxygen permeation fluxes through three-layer BSCF membranes on oxygen partial pressure difference at various temperatures. The measurements were performed by Method 1 (A) without supplying gas flow to the membrane surface, and by Method 2 (B) when the permeate-side surface was exposed to Ar–$O_2$ flow.

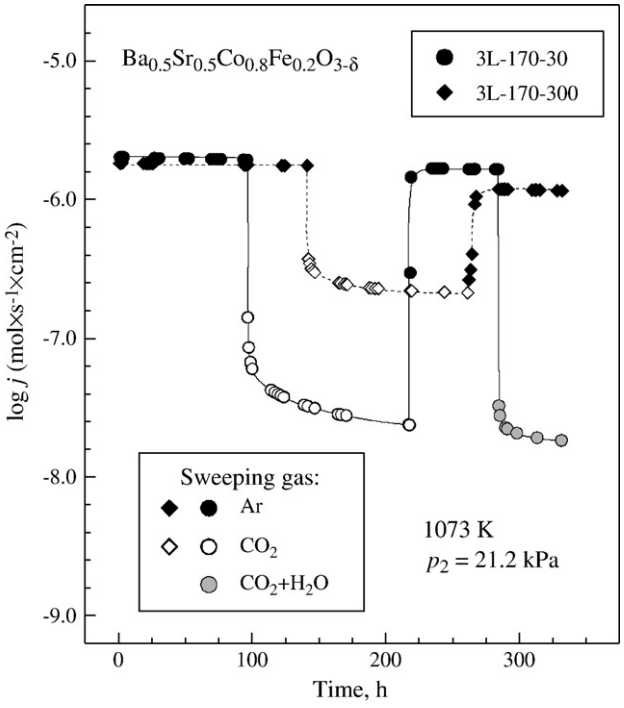


**Fig. 5.** Time dependence of oxygen permeation fluxes through three-layer BSCF membranes exposed to $CO_2$- and $H_2O$-containing atmospheres. Sweeping gas flow rate: 25 cm$^3$/min; $p(O_2)$ in inlet Ar flow: ~10 Pa, $p(O_2)$ in inlet $CO_2$ flow: ~5 Pa, $p(H_2O)$ in inlet ($CO_2 + H_2O$) flow: ~2.6 kPa.

immediately after changing sweep gas (Fig. 5). In particular, at 1073 K asymmetric 3L-170-30 BSCF membrane shows a decrease up to 100 times after changing the permeate-side atmosphere, depending on $CO_2$ or $H_2O$ content. The degradation was almost reversible for the 3L-170-30 membrane, for the 3L-170-300 membrane after switching the gas back to Ar the permeation flux was ~1.5 times lower. SEM inspection of the 3L-170-30 BSCF membrane after the permeation tests showed that the feed-side support surface exposed to air is essentially unchanged (Fig. 2B). On the contrary, a thick porous layer of decomposition products, up to 50 μm, was formed at the permeate-side surface after testing under air/$CO_2$ gradient (Fig. 2C). The observed degradation originates, therefore, from surface decomposition of the membrane due to formation of carbonates and/or hydroxides which almost completely blocks the surface of the thin BSCF porous layer, thus negatively affecting the gaseous oxygen diffusion and desorption in the pores. Apparently, in the case of the 3L-170-300 membrane with a thicker porous layer on the side exposed to $CO_2$/$H_2O$ containing atmospheres, the decomposition process was deeper and resulted in irreversible decrease of the permeation fluxes, on the contrary to the 3L-170-30 membrane. The latter, suggests, in particular, that under realistic conditions of oxygen separation from ambient air containing water and carbon dioxide, an appropriate compromise has to be found between mechanical strength of the membrane supported on the porous layer(s), and their thickness as a factor affecting the oxygen diffusion rate.

## 4. Conclusions

Flat three-layer asymmetric membranes were fabricated by a three-stage uniaxial compaction procedure. The thicknesses of the thick porous support and the dense layer were fixed, whilst the thickness of the thin porous layer was varied from 30 to 300 μm. The characterization techniques for asymmetric membranes as well as for dense and porous components, separately, included X-ray diffraction (XRD) analysis, scanning electron microscopy coupled with energy-dispersive spectroscopy (SEM/EDS), mercury intrusion porosimetry, gas-tightness tests and determination of oxygen permeation fluxes by two experimental techniques. A microstructural engineering approach comprising a three-layer architecture of planar BSCF membrane leads to insignificant increase in oxygen fluxes. At the same time, the formation of three-layer membranes leads to an appearance of important permeation-limiting factor, namely gas diffusion in the porous layers. Stable performance of the asymmetric BSCF membranes can be achieved using an inert sweep gas. In $CO_2$/$H_2O$ containing atmospheres a dramatic decrease in oxygen permeation was observed due to formation of carbonates and/or hydroxides on the surface of thin porous layer.

## Acknowledgements

This work was supported by the by the Belgian Federal Science Policy Foundation (FOD Science policy) and the FCT, Portugal (projects PTDC/CTM/64357/2006 and SFRH/BD/45227/2008). Experimental assistance of J.-P. Moreels, J.F.C. Cooymans, R. Kemps and M. Mertens (VITO) is gratefully acknowledged.

## References


[1] H.J.M. Bouwmeester, A.J. Burggraaf, in: A.J. Burggraaf, L. Cot (Eds.), Fundamentals of Inorganic Membrane Science and Technology, Elsevier Science, Amsterdam–Lausanne–New York–Oxford–Shannon–Tokyo, 1996, p. 435.
[2] A. Thursfield, I.S. Metcalfe, J. Mater. Chem. 14 (2004) 2475.
[3] M.F. Carolan, P.N. Dyer, US Patent 5534471 (1996).
[4] G. Etchegoyen, T. Chartier, P. Del-Gallo, J. Eur. Ceram. Soc. 26 (2006) 2807.
[5] J. Sunarso, S. Baumann, J.M. Serra, W.A. Meulenberg, S. Liu, Y.S. Lin, J.C. Diniz da Costa, J. Membr. Sci. 320 (2008) 13.
[6] J.F. Vente, W. Haije, Z.S. Rak, J. Membr. Sci. 276 (2006) 178.
[7] W. Jin, S. Li, P. Huang, N. Xu, J. Shi, J. Membr. Sci. 185 (2001) 237.
[8] Z.P. Shao, G.X. Xiong, H. Dong, W.S. Yang, L.W. Lin, Sep. Purif. Technol. 25 (2001) 97.
[9] J.F. Vente, S. McIntosh, W.G. Haije, H.J.M. Bouwmeester, J. Solid State Electrochem. 10 (2006) 581.
[10] B. Wei, Z. Lü, X. Huang, J. Miao, X. Sha, X. Xin, W. Su, J. Eur. Ceram. Soc. 26 (2006) 2827.
[11] P. Zeng, Z. Chen, W. Zhou, H. Gu, Z. Shao, S. Liu, J. Membr. Sci. 291 (2007) 148.
[12] L.A. Chick, L.R. Pederson, G.D. Maupin, J.L. Bates, L.E. Thomas, G.L. Exarhos, Mater. Lett. 10 (1990) 6.
[13] V.V. Kharton, A.A. Yaremchenko, A.V. Kovalevsky, A.P. Viskup, E.N. Naumovich, P.F. Kerko, J. Membr. Sci. 163 (1999) 307.
[14] E.V. Tsipis, M.V. Patrakeev, V.V. Kharton, A.A. Yaremchenko, G.C. Mather, A.L. Shaula, I.A. Leonidov, V.L. Kozhevnikov, J.R. Frade, Solid State Sci. 7 (2005) 355.
[15] V.V. Kharton, A.V. Kovalevsky, A.P. Viskup, J.R. Jurado, F.M. Figueiredo, E.N. Naumovich, J.R. Frade, J. Solid State Chem. 156 (2001) 437.
[16] I.P. Marozau, V.V. Kharton, A.P. Viskup, J.R. Frade, V.V. Samakhval, J. Eur. Ceram. Soc. 26 (2006) 1371.
[17] A.A. Yaremchenko, V.V. Kharton, M. Avdeev, A.L. Shaula, F.M.B. Marques, Solid State Ionics 178 (2007) 1205–1217.
[18] V.V. Kharton, E.V. Tsipis, A.A. Yaremchenko, I.P. Marozau, A.P. Viskup, J.R. Frade, E.N. Naumovich, Mater. Sci. Eng. B 134 (2006) 80.
[19] M.V. Patrakeev, I.A. Leonidov, V.L. Kozhevnikov, V.V. Kharton, Solid State Sci. 6 (2004) 907.
[20] V.V. Kharton, A.A. Yaremchenko, E.N. Naumovich, J. Solid State Electrochem. 3 (1999) 303.
[21] Y. Li, E.R. Maxey, J.W. Richardson, J. Am. Ceram. Soc. 88 (2005) 1244.
[22] R.Y. Muydinov, M.N. Popova, A.R. Kaul, Dokl. Chem. 402 (2005) 88.
[23] Yu.D. Tretiakov, Chemistry of Nonstoichiometric Oxides, Moscow State University, Moscow, 1974.
[24] H.S. O'Neill, M.I. Pownceby, Contrib. Mineral. Petrol. 114 (1993) 296.